Nanoscale

PAPER

View Article Online
View Journal | View Issue

Open Access Article. Published on 09 September 2024. Downloaded on 5/21/2026 4:00:45 AM.
This article is licensed under a Creative Commons Attribution 3.0 Unported Licence.

Check for updates

Cite this: *Nanoscale*, 2024, **16**, 18620

Nanoparticle-enabled integration of air capture and conversion of CO_2†

Huanqin Guan,[a] Ju Ye Kim,[b] Kecheng Wei,[a] Mayank Agrawal,[b] Andrew A. Peterson *[b] and Shouheng Sun *[a]

Received 15th July 2024,
Accepted 9th September 2024

DOI: 10.1039/d4nr02925a

rsc.li/nanoscale

Integrating air capture and conversion of CO_2 is key to realizing energy sustainability. However, current integration approaches require high temperature and pressure, making them energy intensive. Here, we demonstrate a nanoparticle (NP) catalysis approach for the hydrogenation of alkyl carbonate, an intermediate obtained from the CO_2 capture process, to formate, achieving one-pot air capture and conversion of CO_2 under ambient conditions. The capture is realized in an ethylene glycol (EG) solution of KOH (EG–KOH) at room temperature, where CO_2 is selectively converted into HO–CH_2CH_2–O–COOK (~100% conversion). This carbonate is then hydrogenated using ammonia borane (under ambient pressure and at 50 °C) to formate (HCOOK) (>90% yield) in the presence of a stable Pd NP catalyst with EG being regenerated. Atomistic simulations suggest that the CO_2 absorption process in the EG–KOH solution is energetically stable, and the catalyst surface provides the reaction site to break the C–O bond in the –O–COOK structure, enabling the hydrogenation of the alkyl carbonate to formate and the regeneration of EG. Our study provides a promising NP-catalysis approach for air capture and conversion of CO_2 into value-added chemicals/fuels under ambient conditions.

Introduction

Energy-efficient air capture and conversion of CO_2 is a promising solution to combat climate change and build an energy-sustainable future.[1–5] The key to the success of this approach is the energy-efficient integration of the capture/conversion processes,[6,7] a goal that has been extremely challenging to achieve. Past approaches for this integration include CO_2 capture by an amine to form a carbamate, followed by catalytic hydrogenation of the carbamate to formate,[8–11] or by an alkaline (KOH) solution to form alkyl carbonate, followed by catalytic hydrogenation to methanol.[12–17] In all these studies, the hydrogenation step is performed under high pressure and temperature conditions and the conversion is catalyzed by homogeneous Ru-pincer hydride complexes.[18–23] To realize the energy-efficient integration of CO_2 capture and conversion, a stable and recyclable catalytic system should be present, which can activate and convert the alkyl carbonate into a valuable chemical or fuel under ambient conditions.

Nanoparticles (NPs) have been studied extensively for catalytic applications. Herein, we report a Pd nanoparticle (NP)-enabled approach for air capture and conversion of CO_2 under ambient conditions, as summarized in Scheme 1. The key idea of our approach is first to capture CO_2 in an ethylene glycol (EG) solution of KOH to convert CO_2 into alkyl carbonate and then to reduce this alkyl carbonate *in situ* to formate *via* Pd NP-catalyzed transfer hydrogenation of ammonia borane (NH_3BH_3, AB) with EG being regenerated. Previous studies have shown that pure CO_2 may be hydrogenated by a metal borohydride or AB in the presence of a special pincer complex as a catalyst,[24–28] but such a hydrogenation reaction is not suitable for the desired one-step air capture and conversion process. We found that Pd NPs were active in catalyzing the AB hydrogenation of alkyl carbonate to formate under ambient pressure. The reaction led to full conversion (100%) of alkyl carbonate and high yield (92%) formation of formate in a 6 h reaction period at 50 °C. The process can be readily applied to integrate air capture and conversion of CO_2 into formate. The Pd NPs are stable in the one-pot capture/conversion process and can be reused for the next capture and conversion step. This NP-catalysis enabled one-pot approach demonstrates a potential energy-efficient integration of air capture and conversion of CO_2 into value-added chemicals/fuels.

[a]*Department of Chemistry, Brown University, Providence, Rhode Island, 02912, USA. E-mail: ssun@brown.edu*
[b]*School of Engineering, Brown University, Providence, Rhode Island 02912, USA. E-mail: Andrew_Peterson@brown.edu*

† Electronic supplementary information (ESI) available. See DOI: https://doi.org/10.1039/d4nr02925a

This journal is © The Royal Society of Chemistry 2024

Open Access Article. Published on 09 September 2024. Downloaded on 5/21/2026 4:00:45 AM.
This article is licensed under a Creative Commons Attribution 3.0 Unported Licence.

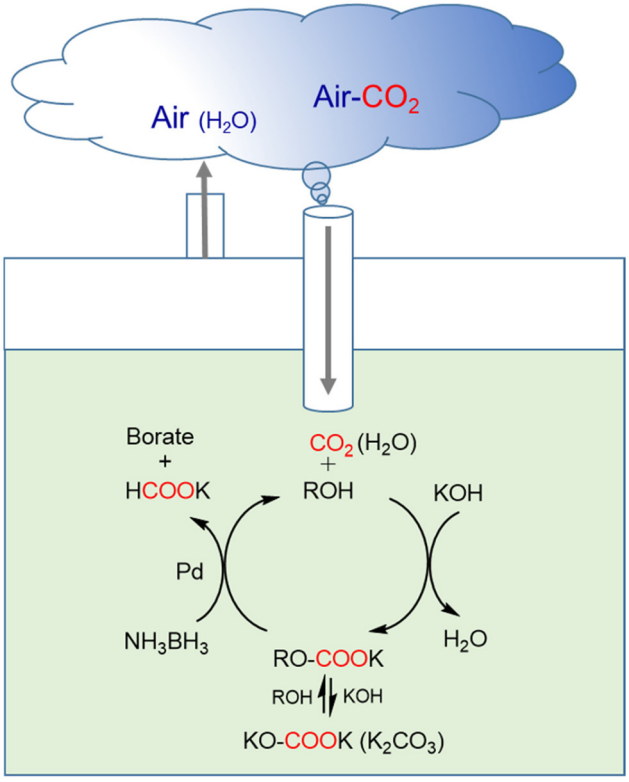

Scheme 1 Illustration of the integrated air capture and conversion of CO_2 into formate under ambient conditions.

Methods and materials

Materials

Palladium acetylacetonate ($Pd(acac)_2$, 99%) and hydrogen tetrachloroaurate(III) hydrate ($HAuCl_4{\cdot}3H_2O$, 99.9%) were purchased from Strem Chemicals. Potassium hydroxide (99%), potassium bicarbonate (99%), potassium carbonate (99%), ammonia borane (90%), oleylamine (technical grade, 70%), borane-*tert*-butylamine (97%), triisopropylsilane (TIPS, 99%), ethylene glycol (anhydrous, 99.8%) and 1-methyl-2-pyrrolidinone (NMP, 99.5%) were purchased from Sigma Aldrich. d_6-DMSO was used as received. Hexane (98.5%), isopropanol (100%), ethanol (100%), *N*,*N*-dimethylformamide (99.8%), and acetic acid (98%) were purchased from Fisher Scientific. The platinum wire (0.5 mm diameter, Premion, 99.997%) and Toray carbon paper (TGP-H-60) were from Alfa Aesar. Polyvinylidene fluoride (PVDF) was from MTI Corporation. Deionized water was from a Millipore Autopure system. All chemicals were used without further purification. Nitrogen (99.99%) and carbon dioxide (99.9999%) were purchased from Corp Brothers, Inc.

Experimental procedures

Pd nanoparticle (NP) synthesis

5 nm Pd NPs were synthesized by modifying a previously reported method.[29] 0.150 g of $Pd(acac)_2$ and oleylamine (15 mL) were added into a three-necked flask and then degassed with nitrogen at 60 °C for 30 min. 0.300 g of borane *tert*-butylamine was dispersed in 4 mL of oleylamine by vortexing and shaking. The temperature of the Pd precursor solution was lowered to and maintained at 40 °C. The solution of borane-*tert*-butylamine was injected into the reaction flask quickly, and within one minute the color of the solution changed to dark brown-black. The temperature was raised to 90 °C at a ramp rate of 3–5 °C min^{-1}. The solution was maintained at 90 °C for 1 h. The NPs were precipitated by adding 100 mL of ethanol and separated by centrifugation at 9000 rpm for 8 min. The NPs were then washed twice with ~75 mL of 1 : 9 hexane : ethanol (9000 rpm for 8 min). The NPs were redispersed in hexane for storage. The subsequent catalyst loading and the activation step are presented in the ESI.†

Direct air capture of CO_2 and *in situ* hydrogenation reaction

5 mmol of KOH was dissolved in 10 mL of EG. A water aspirator was used to create a partial vacuum in the reaction system so that ambient air (~413 ppm CO_2) could continuously bubble through the capture solution. The flow rate was controlled to be 0.2 L min^{-1}. The solution pH was monitored during the capture process to determine the CO_2 saturation point. After 48 hours of bubbling, the solution volume increased by about 3 mL due to moisture in the air. The capture solution was then purged with N_2 to remove gas impurities. Next, 10 mg of Pd/C catalysts and 100 mg of ammonia borane were added to the solution, which was sealed using a balloon. The reaction mixture was maintained at 50 °C for 24 hours. Both gas and liquid products were subjected to GC and NMR analysis, respectively.

The hydrogenation reaction could also be performed under air without N_2 purging, yielding a similar reaction result.

All other electrochemical reaction procedures, characterization methods and computational details are given in the ESI.†

Results and discussion

To study the activation of alkyl carbonate, we first reacted pure CO_2 with an ethylene glycol (EG) solution of KOH to form HO–CH_2CH_2–O–COOK. This alkaline chemistry leading to efficient CO_2 capture has been well-known.[7,12,13] In this study, we bubbled CO_2 from its gas cylinder into the EG solution of KOH at room temperature. In the alkaline EG solution, EG can react with KOH to form a glycoxide anion and water, quickly reaching equilibrium. Upon exposure to CO_2 at room temperature, this equilibrium is shifted to the right, as CO_2 reacts with the glycoxide to form alkyl carbonate (Fig. 1A). This CO_2 absorption process reaches its saturation point once KOH is consumed. We monitored solution pH and product formation to determine the endpoint of the capture process as well as the CO_2 capture capacity. As shown in Fig. 1B, the initial pH of the EG solution of KOH (5 mmol KOH dissolved in 10 mL EG) is around 10.7. Upon CO_2 bubbling, the pH gradually decreased

Open Access Article. Published on 09 September 2024. Downloaded on 5/21/2026 4:00:45 AM.
This article is licensed under a Creative Commons Attribution 3.0 Unported Licence.

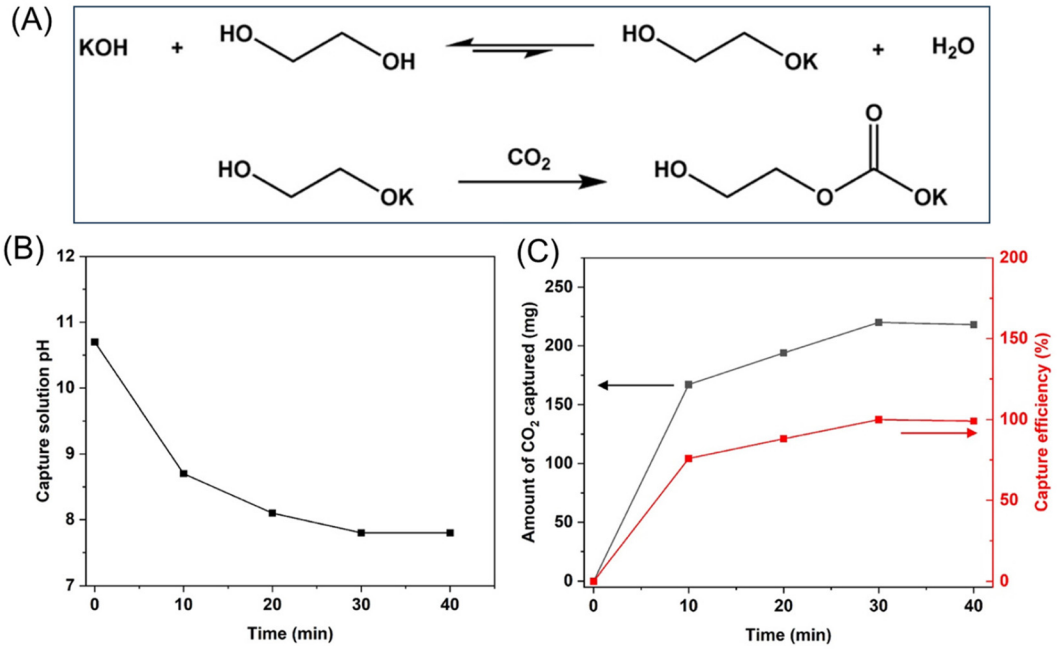

Fig. 1 (A) CO_2 capture by KOH–EG solution. Capture conditions: KOH (5 mmol), EG (10 mL), r.t., and t = 40 min. (B) pH change of capture solution during CO_2 bubbling. (C) The amount of captured CO_2 and capture efficiency during CO_2 bubbling.

and reached a plateau of 7.8 after 40 min. The CO_2 capture capacity of this KOH solution at saturation was measured using the weight change of the solution before and after capture, which was determined to be 220 mg gravimetrically. The capture efficiency can reach nearly 100%, which corresponds to 1 mol CO_2 per mol KOH (Fig. 1C). The alkyl carbonate formed in the EG solution is stable after the capture process and can be quantitatively characterized by both ^{1}H and ^{13}C nuclear magnetic resonance (NMR) spectroscopy, which is consistent with the weight change (Fig. S1†). In this capture process, the amount of KOH is the limiting factor, which determines the maximum amount of CO_2 the system can capture.

The alkyl carbonate could not be activated and reduced by a common hydride agent (AB or sodium borohydride) under atmospheric pressure and at temperatures ranging from room temperature to 80 °C we screened. However, when we studied NP catalysis for transfer hydrogenation of AB, we found Pd NPs to be more active in catalyzing the hydrogenation of alkyl carbonate to formate at 50 °C. We prepared 5 nm Pd NPs *via* solution phase reduction of Pd(acac)$_2$ with borane *t*-butylamine in oleylamine.[29] Fig. S2A† shows the transmission electron microscopy (TEM) image of the 5 nm Pd NPs obtained from the synthesis. The NPs were then loaded onto carbon support, followed by an acetic acid wash to remove the surfactant oleylamine as reported.[30] The TEM image showed that the Pd NPs are well-dispersed on the carbon support after this treatment, showing no sign of aggregation (Fig. S2B†). The Pd NPs have a typical fcc structure as characterized by X-ray diffraction (XRD) (Fig. S2C†). We studied the reduction of alkyl carbonate by AB in the capture solution in the presence of a Pd NP catalyst (Fig. 2A and ESI†). We used a balloon to seal the reaction vessel to ensure that the reaction proceeded under ambient pressure. The conversion of alkyl carbonate was monitored by ^{1}H NMR using dimethylformamide as an internal standard in d$_6$-DMSO solvent. A small amount of aliquot was taken for analysis at each hour time mark. The alkyl carbonate conversion increased with reaction time and reached 100% after 6 h of reaction (Fig. 2B). In the solution phase, formate was the only product characterized by both ^{1}H and ^{13}C NMR (Fig. S3†). The time-dependent formate yield during the reaction is shown in Fig. 2C, reaching its maximum of 92% after 6 h with a turnover frequency (TOF) of 0.059 s^{-1}. The rest of the products contained small amounts of CO and CH_4 as detected by gas chromatography, with CO at 6% and CH_4 at 2%, which might be the result of the deep reduction of the adsorbed formate on the Pd surface, similar to what has been reported for CO_2/formate reduction to CO/CH_4 on a Pd–Al_2O_3 surface.[31] We also detected the formation of H_2 in the reaction system, which is the result of the competing reaction, alcoholysis of AB, under the transfer hydrogenation reaction conditions. Temperature-dependent studies showed that increasing the reaction temperature to 80 °C caused the formate yield to drop, which is due to the exothermic nature of the hydrogenation reaction,[32] while decreasing the temperature to 20 °C also reduced the formate yield due to the slow kinetics (Fig. 2C). When the catalyst loading was doubled to 0.2 mol%, the formate yield did not change much under the same reaction conditions. Without the Pd NP catalyst, however, the formate yield was only 12% even after 48 h of reaction (Table S1†), suggesting that pure AB is not active enough to reduce alkyl carbonate. Our further control experiments

 This journal is © The Royal Society of Chemistry 2024

Open Access Article. Published on 09 September 2024. Downloaded on 5/21/2026 4:00:45 AM.
This article is licensed under a Creative Commons Attribution 3.0 Unported Licence.

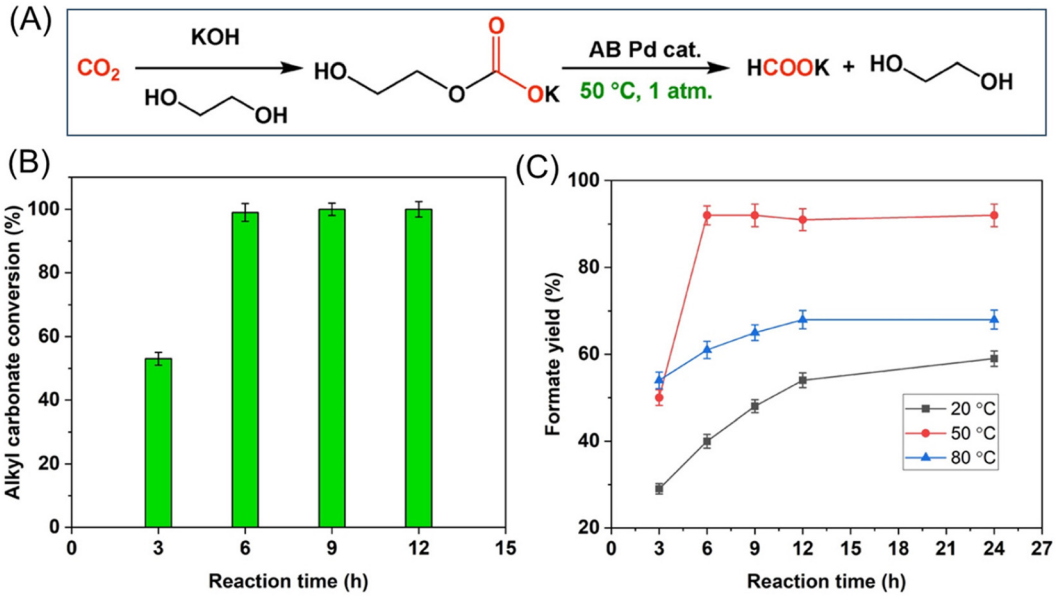

Fig. 2 (A) Integrated CO_2 capture and conversion scheme. (B) Time dependent alkyl carbonate hydrogenation reaction at 50 °C showing carbonate conversion. (C) Temperature effect on the alkyl carbonate hydrogenation showing formate yield. Reaction conditions: solutions from the capture step were directly used for hydrogenation. Alkyl carbonate: 2.0 mmol, ammonia borane (AB): 1.0 mmol, Pd nanocatalyst: 0.1 mol%, and ambient pressure. Formate yields were determined by ^{1}H NMR, and the average value was reported based on three independent experiments.

showed that alkyl carbonate is stable in the reaction solution without AB and Pd NPs, even under heating at 120 °C (Fig. S4†). Additionally, without alkyl carbonate, the reaction of AB and Pd NPs in EG only yielded H_2 that is generated from the Pd-catalyzed solvolysis of AB in EG, similar to what has been extensively reported regarding NP-catalyzed hydrolysis/alcoholysis of AB to generate H_2.[33–35] We further investigated the Pd-catalyzed hydrogenation reaction in the presence of $NaBH_4$ and obtained a similar formate yield. However, atmospheric H_2 was not active enough for the hydrogenation process as the formate yield was only 7% (Table S2†). This indicates that under our current reaction conditions, a hydride intermediate, not a free H_2 molecule, is an active species in the Pd NP-catalyzed hydrogenation of alkyl carbonate to formate.

The formation of potassium carbonate (K_2CO_3) and/or bicarbonate ($KHCO_3$) is inevitable when water and KOH are present in the capture solution. We further studied how the formation of $K_2CO_3/KHCO_3$ affects the AB transfer hydrogenation of alkyl carbonate. We found that both K_2CO_3 and $KHCO_3$ could be dissolved in EG and further reduced by AB in the presence of Pd NPs to formate (87% and 91% yield, respectively) (Fig. 3). This finding is significant for the successful air capture and conversion of CO_2, as it makes the hydrogenation of $K_2CO_3/KHCO_3$ possible without high energy input (inorganic carbonate is generally considered inactive and can only be reduced under harsh conditions[36,37]). Under our reaction conditions, EG plays an important role in activating $K_2CO_3/KHCO_3$ by forming alkyl carbonate, as confirmed by NMR of the precursor solution containing $K_2CO_3/KHCO_3$ and EG (Fig. S5†). This suggests that there exists an equilibrium between carbonate and alkyl carbonate. To further support

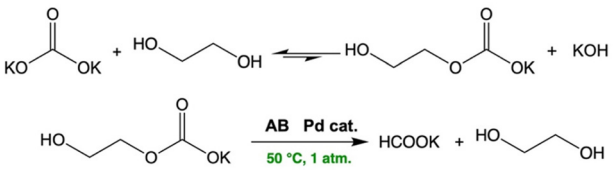

Entry	Carbon source	Solvent	Formate yield (%)
1	Captured CO_2	Ethylene glycol	92
2	$KHCO_3$	Ethylene glycol	91
3	K_2CO_3	Ethylene glycol	87
4	K_2CO_3	H_2O	6

Fig. 3 Investigation of inorganic carbonate/bicarbonate hydrogenation under mild conditions. Reaction conditions: carbonate/bicarbonate (2.0 mmol), EG (10 mL), AB (1.0 mmol), Pd nanocatalyst (0.1 mol%), ambient pressure, 50 °C and 6 h.

this point, we performed $K_2CO_3/KHCO_3$ reduction in an aqueous solution without EG under the same conditions, and we could only detect a very small amount of formate (<6% yield). Therefore, we conclude that EG reacts with carbonates to form alkyl carbonate, reaching equilibrium. Under the Pd NP-catalyzed AB hydrogenation conditions, alkyl carbonate is reduced to formate, which shifts the equilibrium to the right until carbonates are consumed. This indicates that water in the EG/KOH solution only slows down the hydrogenation process, but does not affect the final reaction outcome, which is key to continuous air capture and conversion of CO_2.

Our model study on pure CO_2 capture and conversion in EG–KOH solution as well as the EG role in activating K_2CO_3/

Open Access Article. Published on 09 September 2024. Downloaded on 5/21/2026 4:00:45 AM.
This article is licensed under a Creative Commons Attribution 3.0 Unported Licence.

$KHCO_3$ motivated us to further explore CO_2 capture from air, where moisture is also ubiquitously present. The capture and conversion system and the related reactions are outlined in Scheme 1. A water aspirator was used as a pump to draw ambient air into the capture solution, in which ultra-dilute CO_2 (~413 ppm) was captured by KOH in EG.[7] The solution pH was monitored throughout the capture process, and it took 48 h for the pH to stabilize (Fig. 4A). The ^{13}C NMR analysis of the capture product shows an additional peak of CO_3^{2-} (165.70 ppm) in addition to the presence of alkyl carbonate (Fig. 4B and C). The CO_3^{2-} species must be formed from reactions among water (from the air), KOH, and CO_2. Based on the quantitative ^{13}C NMR analysis, the ratio between alkyl carbonate and K_2CO_3 was about 1 : 1. When the air capture solution was hydrogenated by AB at 50 °C in the presence of the Pd NP catalyst for 24 h, all carbonates were converted into formate (91% yield). Compared with the result observed from the pure CO_2 capture and conversion demonstrated above, the hydrogenation of carbonates from air capture requires a longer reaction time due to the less efficient conversion of inorganic carbonate into alkyl carbonate in the presence of water. Another highlight of our reaction system is that the Pd NP-catalyzed transfer hydrogenation is O_2 tolerant – the reaction can proceed without the need to purge the reaction system with N_2 to remove O_2. As a comparison, O_2 must be removed from the reaction system under conventional hydrogenation reaction conditions.[2,7,12] Finally, the Pd NPs showed excellent stability under the catalytic transfer hydrogenation reaction conditions and maintained a formate yield of over 90% after 5 reaction cycles (Fig. 4D) (the same amounts of AB and KOH were added in each reaction cycle). The Pd NPs retain their crystal structure (Fig. S6A†) and NP size/dispersity (Fig. S6B†) as confirmed by the XRD and TEM analyses of the NPs before and after the catalytic reactions, indicating the long-term stability of the Pd NPs as an efficient catalyst for continuous air capture and conversion.

To understand why Pd NPs are efficient for the AB hydrogenation of alkyl carbonate, we used density functional theory (DFT) calculations to further investigate the reaction mechanism on Pd surfaces. We suggest a 5-step mechanism, starting with the incorporation of CO_2 into a solution of KOH in EG, as shown in Fig. 1. Given that the Pd NPs are nano-sized polyhedra (~5 nm) (Fig. S2†), which means that they consist of many step and terrace sites, both the planar (111) and the stepped (211) crystal facets of Pd were examined using DFT calculations, as shown in Fig. S9.† This comparison shows a more facile route on the (211) step edge than on the (111) terrace, and we highlight the (211) results herein.

The overall suggested reaction mechanism and the corresponding Gibbs free energies are summarized in Fig. 5, where "*" represents an adsorbed species on the Pd surface. State 1 → state 2 represents the formation of an EG–CO_2 complex

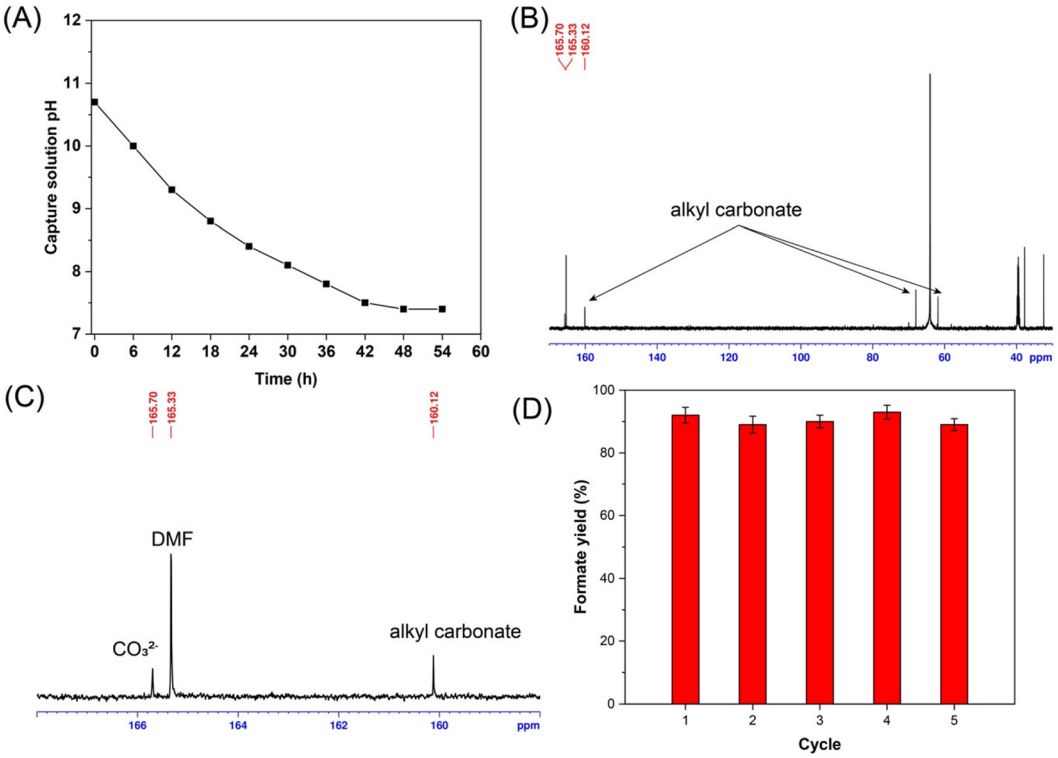

Fig. 4 (A) Capture solution pH change in the direct air capture process. (B) ^{13}C NMR spectra of CO_2 captured from lab air in d_6-DMSO. (C) Enlargement of Fig. 4B showing carbonyl peaks for alkyl carbonate and CO_3^{2-}. (D) Catalytic stability of formate yields after 5 consecutive catalytic cycles. Reaction conditions: KOH (5 mmol), EG (10 mL), AB (2.0 mmol), Pd nanocatalyst (0.1 mol%), ambient pressure, and 50 °C.

 This journal is © The Royal Society of Chemistry 2024

Open Access Article. Published on 09 September 2024. Downloaded on 5/21/2026 4:00:45 AM.
This article is licensed under a Creative Commons Attribution 3.0 Unported Licence.

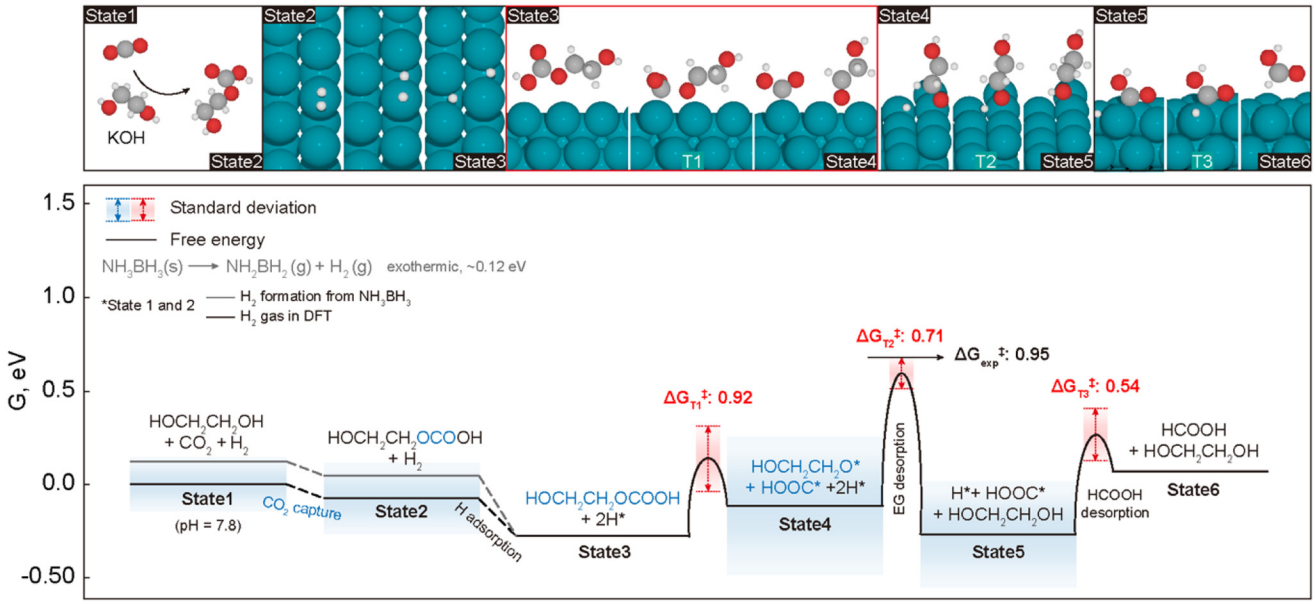

Fig. 5 The schemes at the top of the graph show the reaction process, with the red, gray, white, and cyan atoms in the schemes representing O, C, H, and Pd, respectively. Bottom shows the free energy diagram for formic acid (HCOOH) formation by EG and CO_2 at 50 °C and 1 atm. The *y*-axis represents the Gibbs free energy (*G*, eV), and the Gibbs free energy of activation $\left(\Delta G^{\ddagger}_{Tx}\right)$ is shown (red color) inside the graph. Free energy diagram with error estimation (blue gradient box for each state) obtained from the BEEF ensembles. The free energy required for H_2 production from NH_3BH_3 is shown in gray for state 1 and state 2.

under the pH 7.8 environment; we considered the pH effect in state 1 because protons are involved in the reaction for forming the EG–CO_2 complex.[38] As expected from the experiments in which alkyl carbonate intermediates were formed immediately when CO_2 was purged, the reaction from state 1 to state 2 proceeds spontaneously with a downhill energy path. While the reaction from state 1 to state 2 takes place without a Pd catalyst, after state 2, the reaction takes place on the surface of the Pd catalyst. Accordingly, each Gibbs energy of activation (reaction energy barrier) from state 3 was calculated to investigate the rate-determining step. T1 is an abbreviation of transition state 1, and a total of 3 transition states (T1, T2, and T3) and each Gibbs energy of activation ($\Delta G^{\ddagger}_{T1}$, $\Delta G^{\ddagger}_{T2}$, and $\Delta G^{\ddagger}_{T3}$, respectively) were calculated by the dynamic nudged elastic band (DyNEB) method.[39] We modeled the process of H_2 formation by AB as a process in which H* is adsorbed to Pd from H_2 (state 2 → state 3), and this process is a thermodynamically easy reaction with a downhill energy profile. Considering the consistency in the calculation environment, we started the reaction with an H_2 gas molecule represented by a black color bar, while also showing the reaction energy for generating H_2 from NH_3BH_3 in a gray color bar to account for the use of NH_3BH_3 in the actual experiments. The theoretical Gibbs energy of activation $\left(\Delta G^{\ddagger}_{\text{theoretical}} = 0.88\,\text{eV}\right)$ was calculated as the free energy change between state 3 (the lowest-energy state) and transition state 2 (the highest-energy barrier), which suggests that the rate-determining step of this reaction is the hydrogenation and release of EG ($HOCH_2CH_2OCOO^-$ + H* → $HOCH_2CH_2OH$). Considering that the experimental turnover frequency (TOF) is 0.059 s^{-1}, we can estimate that $\Delta G^{\ddagger}_{\text{exp}}$ (Gibbs energy for the experimental activation) is around 0.95 eV from the Eyring equation:

$$\text{Rate constant} = \frac{\kappa \times k_B T}{h}\, e^{\frac{-\Delta G^{\ddagger}}{RT}}$$

where κ is the transmission coefficient, which was assumed to be 1 in this study, $\Delta G^{\ddagger}$ is the Gibbs energy of activation, k_B is Boltzmann's constant, T is the temperature, h is Planck's constant, and R is the gas constant.

Although the DFT-calculated barriers were close to the experimental barrier, we wanted to understand if the deviation was reasonable. We predicted errors from the ensemble-based Bayesian error estimation functional (BEEF) (Fig. 5, see the blue and red gradient box),[40] where the calculated $\Delta G^{\ddagger}_{\text{theoretical}}$ was in the range between 0.80 eV and 0.95 eV, as shown in Fig. 5. Given the error in any experimental measurement, we consider the experimental and calculated barriers to be indistinguishable.

After the breakage of the intermediate product and adsorption on the Pd surface (state 4), a hydrogenation reaction proceeds to produce EG and HCOOH. State 4 → state 5 represents the production of recycled EG, and state 5 → state 6 is an HCOOH production step. As a result, it was confirmed that the CO_2 absorption process in the solution of KOH in EG is energetically stable (state 1 → state 2), and the major role of the Pd catalyst is to break the C–O bond of the alkyl carbonate intermediate (state 3 → state 4), as well as to provide a reservoir of hydride for product release.

We also tested if the direct air capture system can be coupled with electrocatalysis to reduce alkyl carbonate without

Open Access Article. Published on 09 September 2024. Downloaded on 5/21/2026 4:00:45 AM.
This article is licensed under a Creative Commons Attribution 3.0 Unported Licence.

the use of AB. In our preliminary studies, Pd NPs were active in catalyzing the electrochemical reduction of alkyl carbonate to formate, but the reduction at the catalyst surface produced formate at too low a concentration to detect. Instead of pursuing the reduction to a liquid product, we tested the reduction to a gaseous product that can be easily separated from the reaction system and characterized. Since Au nanowires are known to be active to electro-catalyze CO_2 to CO,[41] we prepared 2 nm ultra-thin Au nanowires (Fig. S7†) and studied their catalysis for the electrochemical reduction of alkyl carbonate in the capture solution (EG/H_2O v/v ~ 5/1) (Fig. S8†). At −1.4 V (*vs.* Ag/AgCl), the CO faradaic efficiency reached 21% with H_2 as the side product. An important point to note is that carbonate/bicarbonate cannot be reduced under common electrochemical CO_2 reduction conditions,[42] and some studies suggest that the electrochemical conversion of carbonates from direct air capture solution could be attributed to the acidification of the carbonates to CO_2 at the bipolar membrane interface.[43] We are currently working on demonstrating nanocatalysts for efficient electro-reduction of alkyl carbonate as a new approach for the integration of direct air capture and conversion of CO_2 into value-added chemicals.

Conclusions

This report demonstrates an NP-catalyzed hydrogenation of carbonates to realize the integration of air capture and conversion of CO_2 into formate. The key concept is to fast capture CO_2 from the air *via* a strong alkaline solution of EG–KOH, converting the CO_2 into alkyl carbonate $HOCH_2CH_2O$–COOK. This carbonate is stable in the capture medium and can be characterized and quantified. More importantly, the alkyl carbonate can be further activated by Pd NPs and then hydrogenated by AB (100% conversion) to formate (>90% yield) under ambient pressure and 50 °C with EG being regenerated. The formation of carbonate/bicarbonate salts from the air (moisture) capture process only affects the reaction kinetics, not the overall reaction outcome due to the established equilibrium among carbonates, EG, and alkyl carbonate. Without EG, these carbonates cannot be easily hydrogenated, demonstrating the important role of EG in promoting the hydrogenation of carbonates. DFT calculations suggest that the (211) step edge exposure on the Pd NP surface is especially active for promoting the carbonate hydrogenation reaction. The Gibbs free energy diagram shows a 5-step reaction mechanism for the CO_2 capture and conversion process, and the rate-determining step is the hydrogenation and release of EG. After incorporating the solvation effect, the calculated theoretical activation barriers match well with the experimental ones. Our studies provide a promising approach for the continuous air capture of CO_2 and subsequent formate synthesis. Our preliminary tests also show that it is possible to use an NP catalyst to activate the alkyl carbonate electrochemically. We are working to develop a robust electrocatalyst system to selectively convert this alkyl carbonate into value-added chemicals/fuels and to realize energy-efficient integration of direct air capture and conversion of CO_2 for green and sustainable energy applications.

Data availability

The data supporting this article are available within the main article as well as its ESI.†

Conflicts of interest

The authors declare no conflict of interest.

Acknowledgements

This work was supported by the NSF under Grants CHE-2102290 and CBET-2324345 and by Brown University's Office of Vice President for Research. Electronic structure calculations were carried out at the Brown University Center for Computation and Visualization (CCV).

References

1 E. S. Sanz-Pérez, C. R. Murdock, S. A. Didas and C. W. Jones, Direct Capture of CO_2 from Ambient Air, *Chem. Rev.*, 2016, **116**(19), 11840–11876.
2 M. Erans, E. S. Sanz-Pérez, D. P. Hanak, Z. Clulow, D. M. Reiner and G. A. Mutch, Direct air capture: process technology, techno-economic and socio-political challenges, *Energy Environ. Sci.*, 2022, **15**(4), 1360–1405.
3 S. De, A. Dokania, A. Ramirez and J. Gascon, Advances in the Design of Heterogeneous Catalysts and Thermocatalytic Processes for CO_2 Utilization, *ACS Catal.*, 2020, **10**(23), 14147–14185.
4 X. Jiang, X. Nie, X. Guo, C. Song and J. G. Chen, Recent Advances in Carbon Dioxide Hydrogenation to Methanol via Heterogeneous Catalysis, *Chem. Rev.*, 2020, **120**(15), 7984–8034.
5 K. Wei, H. Guan, Q. Luo, J. He and S. Sun, Recent advances in CO_2 capture and reduction, *Nanoscale*, 2022, **14**(33), 11869–11891.
6 I. Sullivan, A. Goryachev, I. A. Digdaya, X. Li, H. A. Atwater, D. A. Vermaas and C. Xiang, Coupling electrochemical CO_2 conversion with CO_2 capture, *Nat. Catal.*, 2021, **4**(11), 952–958.
7 S. Kar, A. Goeppert and G. K. S. Prakash, Integrated CO_2 Capture and Conversion to Formate and Methanol: Connecting Two Threads, *Acc. Chem. Res.*, 2019, **52**(10), 2892–2903.
8 Y.-N. Li, L.-N. He, A.-H. Liu, X.-D. Lang, Z.-Z. Yang, B. Yu and C.-R. Luan, In situ hydrogenation of captured CO_2 to formate with polyethyleneimine and Rh/monophosphine system, *Green Chem.*, 2013, **15**(10), 2825–2829.

 This journal is © The Royal Society of Chemistry 2024

Open Access Article. Published on 09 September 2024. Downloaded on 5/21/2026 4:00:45 AM.
This article is licensed under a Creative Commons Attribution 3.0 Unported Licence.

9 H.-C. Fu, F. You, H.-R. Li and L.-N. He, CO_2 Capture and *in situ* Catalytic Transformation, *Front. Chem.*, 2019, **7**(525), 1–15.
10 S. Zhang, Y.-N. Li, Y.-W. Zhang, L.-N. He, B. Yu, Q.-W. Song and X.-D. Lang, Equimolar Carbon Absorption by Potassium Phthalimide and In Situ Catalytic Conversion Under Mild Conditions, *ChemSusChem*, 2014, **7**(5), 1484–1489.
11 D. Wei, H. Junge and M. Beller, An amino acid based system for CO_2 capture and catalytic utilization to produce formates, *Chem. Sci.*, 2021, **12**(17), 6020–6024.
12 R. Sen, A. Goeppert, S. Kar and G. K. S. Prakash, Hydroxide Based Integrated CO_2 Capture from Air and Conversion to Methanol, *J. Am. Chem. Soc.*, 2020, **142**(10), 4544–4549.
13 R. Sen, C. J. Koch, A. Goeppert and G. K. S. Prakash, Tertiary Amine-Ethylene Glycol Based Tandem CO_2 Capture and Hydrogenation to Methanol: Direct Utilization of Post-Combustion CO_2, *ChemSusChem*, 2020, **13**(23), 6318–6322.
14 J. Kothandaraman, A. Goeppert, M. Czaun, G. A. Olah and G. K. Surya Prakash, CO_2 capture by amines in aqueous media and its subsequent conversion to formate with reusable ruthenium and iron catalysts, *Green Chem.*, 2016, **18**(21), 5831–5838.
15 M. Scott, B. Blas Molinos, C. Westhues, G. Franciò and W. Leitner, Aqueous Biphasic Systems for the Synthesis of Formates by Catalytic CO_2 Hydrogenation: Integrated Reaction and Catalyst Separation for CO_2-Scrubbing Solutions, *ChemSusChem*, 2017, **10**(6), 1085–1093.
16 S. Kar, R. Sen, A. Goeppert and G. K. S. Prakash, Integrative CO_2 Capture and Hydrogenation to Methanol with Reusable Catalyst and Amine: Toward a Carbon Neutral Methanol Economy, *J. Am. Chem. Soc.*, 2018, **140**(5), 1580–1583.
17 D. Wei, R. Sang, P. Sponholz, H. Junge and M. Beller, Reversible hydrogenation of carbon dioxide to formic acid using a Mn-pincer complex in the presence of lysine, *Nat. Energy*, 2022, **7**(5), 438–447.
18 K. Sordakis, C. Tang, L. K. Vogt, H. Junge, P. J. Dyson, M. Beller and G. Laurenczy, Homogeneous Catalysis for Sustainable Hydrogen Storage in Formic Acid and Alcohols, *Chem. Rev.*, 2018, **118**(2), 372–433.
19 M. D. Porosoff, B. Yan and J. G. Chen, Catalytic reduction of CO_2 by H_2 for synthesis of CO, methanol and hydrocarbons: challenges and opportunities, *Energy Environ. Sci.*, 2016, **9**(1), 62–73.
20 D. B. Lao, B. R. Galan, J. C. Linehan and D. J. Heldebrant, The steps of activating a prospective CO_2 hydrogenation catalyst with combined CO_2 capture and reduction, *Green Chem.*, 2016, **18**(18), 4871–4874.
21 S. Kar, A. Goeppert, V. Galvan, R. Chowdhury, J. Olah and G. K. S. Prakash, A Carbon-Neutral CO_2 Capture, Conversion, and Utilization Cycle with Low-Temperature Regeneration of Sodium Hydroxide, *J. Am. Chem. Soc.*, 2018, **140**(49), 16873–16876.
22 S. Kostera, S. Weber, M. Peruzzini, L. F. Veiros, K. Kirchner and L. Gonsalvi, Carbon Dioxide Hydrogenation to Formate Catalyzed by a Bench-Stable, Non-Pincer-Type Mn (I) Alkylcarbonyl Complex, *Organometallics*, 2021, **40**(9), 1213–1220.
23 R. Bhardwaj, A. Kumar and J. Choudhury, An all-aqueous and phosphine-free integrated amine-assisted CO_2 capture and catalytic conversion to formic acid, *Chem. Commun.*, 2022, **58**(82), 11531–11534.
24 T. Zhao, C. Li, X. Hu, F. Liu and Y. Wu, Base-assisted transfer hydrogenation of CO_2 to formate with ammonia borane in water under mild conditions, *Int. J. Hydrogen Energy*, 2021, **46**(29), 15716–15723.
25 I. Knopf and C. C. Cummins, Revisiting CO_2 Reduction with $NaBH_4$ under Aprotic Conditions: Synthesis and Characterization of Sodium Triformatoborohydride, *Organometallics*, 2015, **34**(9), 1601–1603.
26 L. Lombardo, Y. Ko, K. Zhao, H. Yang and A. Züttel, Direct CO_2 Capture and Reduction to High-End Chemicals with Tetraalkylammonium Borohydrides, *Angew. Chem., Int. Ed.*, 2021, **60**(17), 9580–9589.
27 W. Zhao, H. Li, H. Zhang, S. Yang and A. Riisager, Ammonia borane-enabled hydrogen transfer processes: Insights into catalytic strategies and mechanisms, *Green Energy Environ.*, 2023, **8**, 948–971.
28 Z.-W. Qu, H. Zhu, R. Streubel and S. Grimme, Catalyst-free CO_2 hydrogenation with BH_3NH_3 in water: DFT mechanistic insights, *Phys. Chem. Chem. Phys.*, 2022, **24**(23), 14159–14164.
29 V. Mazumder and S. Sun, Oleylamine-Mediated Synthesis of Pd Nanoparticles for Catalytic Formic Acid Oxidation, *J. Am. Chem. Soc.*, 2009, **131**(13), 4588–4589.
30 D. Li, C. Wang, D. Tripkovic, S. Sun, N. M. Markovic and V. R. Stamenkovic, Surfactant Removal for Colloidal Nanoparticles from Solution Synthesis: The Effect on Catalytic Performance, *ACS Catal.*, 2012, **2**(7), 1358–1362.
31 X. Wang, H. Shi, J. H. Kwak and J. Szanyi, Mechanism of CO_2 Hydrogenation on Pd/Al_2O_3 Catalysts: Kinetics and Transient DRIFTS-MS Studies, *ACS Catal.*, 2015, **5**(11), 6337–6349.
32 J. Su, M. Lu and H. Lin, High yield production of formate by hydrogenating CO_2 derived ammonium carbamate/carbonate at room temperature, *Green Chem.*, 2015, **17**(5), 2769–2773.
33 C. Yu, X. Guo, M. Shen, B. Shen, M. Muzzio, Z. Yin, Q. Li, Z. Xi, J. Li, C. T. Seto and S. Sun, Maximizing the Catalytic Activity of Nanoparticles through Monolayer Assembly on Nitrogen-Doped Graphene, *Angew. Chem., Int. Ed.*, 2018, **57**(2), 451–455.
34 M. Muzzio, H. Lin, K. Wei, X. Guo, C. Yu, T. Yom, Z. Xi, Z. Yin and S. Sun, Efficient Hydrogen Generation from Ammonia Borane and Tandem Hydrogenation or Hydrodehalogenation over AuPd Nanoparticles, *ACS Sustainable Chem. Eng.*, 2020, **8**(7), 2814–2821.
35 H. Guan, M. Shen, C. Harris, H. Lin, K. Wei, M. Morales, N. Bronowich and S. Sun, Cu_2O nanoparticle-catalyzed tandem reactions for the synthesis of robust polybenzoxazole, *Nanoscale*, 2022, **14**(16), 6162–6170.

Open Access Article. Published on 09 September 2024. Downloaded on 5/21/2026 4:00:45 AM.
This article is licensed under a Creative Commons Attribution 3.0 Unported Licence.

36 S. Coufourier, Q. Gaignard Gaillard, J.-F. Lohier, A. Poater, S. Gaillard and J.-L. Renaud, Hydrogenation of CO_2, Hydrogenocarbonate, and Carbonate to Formate in Water using Phosphine Free Bifunctional Iron Complexes, *ACS Catal.*, 2020, **10**(3), 2108–2116.

37 C. Rebreyend, E. A. Pidko and G. A. Filonenko, Homogeneous hydrogenation of saturated bicarbonate slurry to formates using multiphase catalysis, *Green Chem.*, 2021, **23**(22), 8848–8852.

38 J. K. Nørskov, J. Rossmeisl, A. Logadottir, L. Lindqvist, J. R. Kitchin, T. Bligaard and H. Jónsson, Origin of the Overpotential for Oxygen Reduction at a Fuel-Cell Cathode, *J. Phys. Chem. B*, 2004, **108**(46), 17886–17892.

39 P. Lindgren, G. Kastlunger and A. A. Peterson, Scaled and Dynamic Optimizations of Nudged Elastic Bands, *J. Chem. Theory Comput.*, 2019, **15**(11), 5787–5793.

40 J. J. Mortensen, L. B. Hansen and K. W. Jacobsen, Real-space grid implementation of the projector augmented wave method, *Phys. Rev. B: Condens. Matter Mater. Phys.*, 2005, **71**(3), 035109.

41 W. Zhu, Y.-J. Zhang, H. Zhang, H. Lv, Q. Li, R. Michalsky, A. A. Peterson and S. Sun, Active and Selective Conversion of CO_2 to CO on Ultrathin Au Nanowires, *J. Am. Chem. Soc.*, 2014, **136**(46), 16132–16135.

42 O. Gutiérrez-Sánchez, N. Daems, W. Offermans, Y. Y. Birdja, M. Bulut, D. Pant and T. Breugelmans, The inhibition of the proton donor ability of bicarbonate promotes the electrochemical conversion of CO_2 in bicarbonate solutions, *J. CO_2 Util.*, 2021, **48**, 101521.

43 O. Gutiérrez-Sánchez, B. de Mot, N. Daems, M. Bulut, J. Vaes, D. Pant and T. Breugelmans, Electrochemical Conversion of CO_2 from Direct Air Capture Solutions, *Energy Fuels*, 2022, **36**(21), 13115–13123.

 This journal is © The Royal Society of Chemistry 2024